PAPER • OPEN ACCESS

Model approach for electromagnetically excited mechanical vibrations in direct-drive wind turbines

View the article online for updates and enhancements.

Model approach for electromagnetically excited mechanical vibrations in direct-drive wind turbines

Christoph Mülder [1]; Tobias Duda [2]; Georg Jacobs [2]; Kay Hameyer [1]

[1] Institute of Electrical Machines (IEM), Schinkelstr. 4, 52062 Aachen
[2] Center for Wind Power Drives (CWD), Campus Boulevard 61, 52074 Aachen
RWTH Aachen University

christoph.muelder@cwd.rwth-aachen.de
tobias.duda@cwd.rwth-aachen.de

Abstract. In this paper a multi-physical modelling approach for calculating parasitic magnetic force excitations in wind turbine generators is presented. These parasitic excitations are dependent on the magnetic field distribution in the air gap and the air gap geometric shape, which is dependent on the external loads of the wind turbine. With this methodology mechanical multibody simulation is coupled with electromagnetic field calculation by means of finite-element calculation. First the general methodology and the calculation of the air gap width distribution is presented and subsequently the electromagnetic field and force calculation is explained.

1. Motivation

Power production from renewable resources is a cornerstone of the energy supply of the future. Therefore, renewable energy production must become competitive to fossil and nuclear energy sources. One way to approach this is to increase the power density of the turbine, which results in bigger and more complex turbines and drivetrains [1]. This trend for increasing turbine power has led to shorter product development cycles. Therefore, novel and efficient simulation models are required, which generate reliable results in the design process of the drivetrain.

There are several models that can calculate the isolated behaviour of electric machines [2]. In contrast, a validated and applicable approach for modelling the transient, structure-dynamic interaction of electrical machines with the surrounding-system is missing today. Such system analyses are carried out in elastic multibody calculation environments which, according to the current state of the art, do not offer a computationally efficient interface for taking into account the interaction between airgap imperfection due to deformation and electromagnetic air gap forces [3].

This paper introduces an electromechanical simulation method for direct-drive generators, which integrates the parasitic electromagnetic forces in the air gap of the generator in a multi-body simulation model. These parasitic air gap forces excite the generators structural element and cause mechanical vibrations. This may lead to excessive wear or acoustic emission. Therefore, a predictive model of the air gap force distribution during operation is already required in the design process to prevent unwanted turbine behaviour.

2. Methodology

Figure 1 shows the approach for the electromechanical simulation. In the first step an electromagnetic field calculation by means of finite element method (FEM) is performed. The solution from the FEM model is then stored into look-up tables, which will contain the acting forces F on the rotor and stator surfaces.

These forces will be subsequently transferred over to a multibody simulation model of the turbine, which can apply the mechanical rotor loads and weight forces on the structural components of the generator. These acting forces are different for each operation point of the generator, which contains the generator currents I and the rotational speed of the turbine n. As the mechanical model is modelled with elastic bodies, the structural components of the generator will experience deformation and displacements from either wind loads and/or electromagnetic forces (see Figure 1).

The resulting rotor and stator displacement and deformation will change the airgap geometry δ, which consequently will change the flux density distribution in the air gap. This change in air gap flux density will subsequently lead to a different force distribution in the air gap. Therefore, a set of multiple look-up tables is created to account for any rotor angular positions φ and air gap widths δ.

To consider the dynamic interaction between structural elements of the generator and electromagnetic active components, a force-element has to be implemented, which can exert electromagnetic forces on structural elements of the generator. By this force-element the transient excitation of the electromagnetic field can be simulated and further studied.
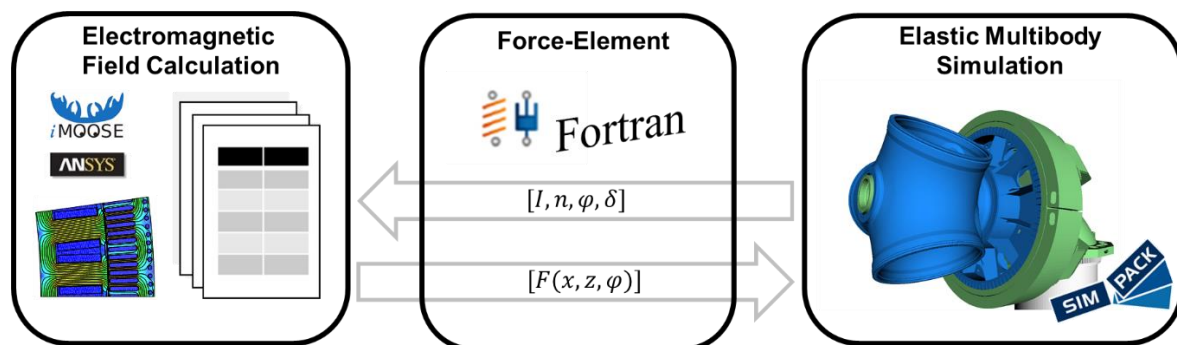
Figure 1: Approach for electromechanical simulation of a direct-drive generator.

3. Mechanical calculation: Air gap width distribution

The force application on the generator structure needs to be implemented via a force-element in the multibody simulation environment (e.g. Simpack). Since the electromagnetic forces are a continuous stress distribution (Maxwell stresses) on the rotor, respectively stator surface, this stress distribution needs to be discretised onto subsurfaces (Figure 2, right). These discretised forces are subsequently applied onto defined points (markers) on the rotor and stator, which will distribute the force equally onto the subsurface. The electromagnetic pull between rotor and stator is decoupled by equivalent internal acting forces pushing rotor outwards and stator inwards, instead of pulling rotor and stator together, see Figure 2. [1]
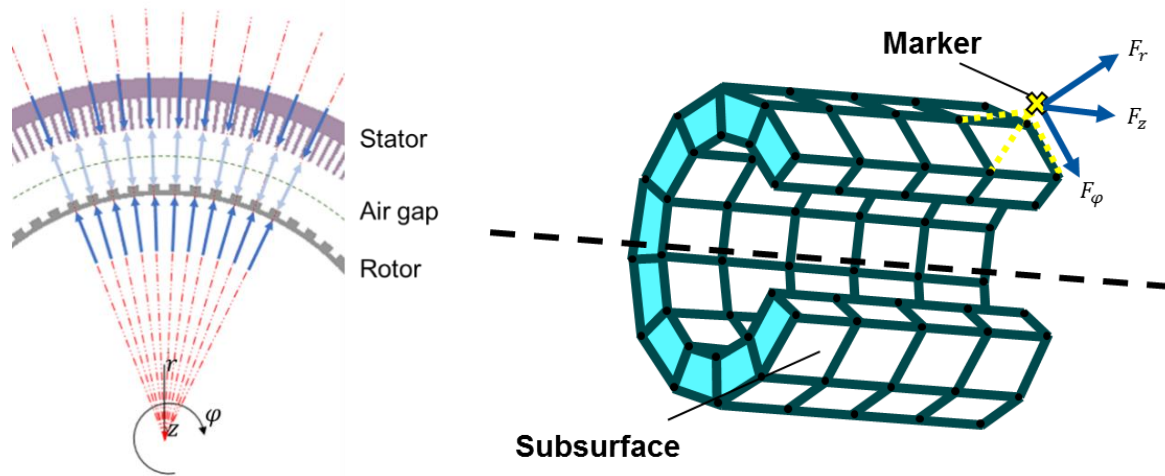
Figure 2:   Acting forces on rotor and stator surface (light blue) and substitute forces (dark blue) [1].

These acting forces are influenced by the air gap width. Locations with an increased air gap width have a lower permeance and therefore experience lower field densities respectively lower forces. This leads to a significant influence of external loads, by means of eccentricities and local deformations, on the field distribution and in turn on the acting forces on rotor and stator. These acting forces generate again eccentricities and local deformations. Due to this interaction between external loads and magnetic forces, rotor and stator needs to be implemented as flexible bodies.[5] In turn, the measurement of the local air gap width is of major importance for a realistic force application.

Since the turbine is exposed to external loads and the drivetrain will deform eventually, there are three rotor displacement states to be considered, shown in Figure 3:

1. Due to the rotation of the drivetrain, there is an angular displacement between rotor and stator
2. External loads (especially weight forces) will lead to tilting between rotor and stator
3. The rotor will be eccentric to the stator

Since the force-element should be universal applicable, the number of rotor and stator markers and therefore the discretisation level of the model, should be freely selectable.

Due to these displacement states a direct measurement of the air gap width and a direct force application between rotor and stator markers is not possible. This is due to the distance between rotor and stator markers (and the airgap width) would change with the position of the respective markers. As stated above, the angular displacement can easily be handled by decoupling rotor and stator by applying equivalent internal forces onto individual markers instead of using forces between rotor and stator markers, see Figure 2. [1]
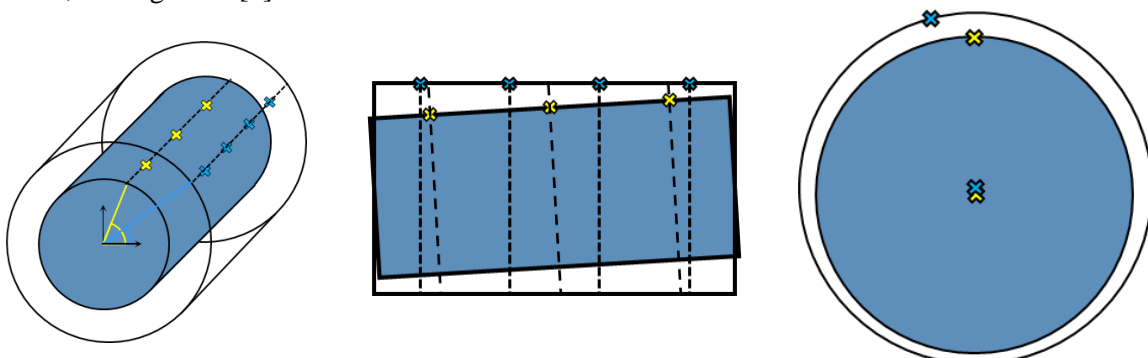
Figure 3:   Schematic view of rotor (dark blue) with rotor markers (yellow) and stator (transparent) with stator markers (bright blue), left: angular displacement between rotor and stator; middle: tilting of rotor inside of the stator; right: rotor eccentricity.

The displacement states of tilting and eccentricities could be handled by calculating the air gap widths by means of cylinder equations. However, this would not consider local deformations of the rotor and stator surface, as the coordinates of the respective marker will not be in the solution room of a cylinder equation. This is exemplarily shown in Figure 4, as S_{S3} is not on the same circle (cylinder surface) as S_{S2}. Therefore, the air gap width will be estimated for each marker individually. For determining the air gap width δ_R for the marker S_R the following process will be used:

1. Select nearest stator surface marker S_{S2} to S_R
2. Determine the stator surface marker S_{S2}' in the projected rotor plane
3. Generate circle equation with S_{S2}' and C_S'
4. Calculate point of intersection S_{S2}''
5. Calculate the distance between S_{S2}'' and S_R which is the air gap widths δ_{R1}

However, this process is still an estimation of the air gap width, as the position of S_{S2}'' is determined with an ideal circle, but it still utilizes the deformation at marker S_{S2}. The calculation error of this method is dependent on the discretization level of the subsurfaces.
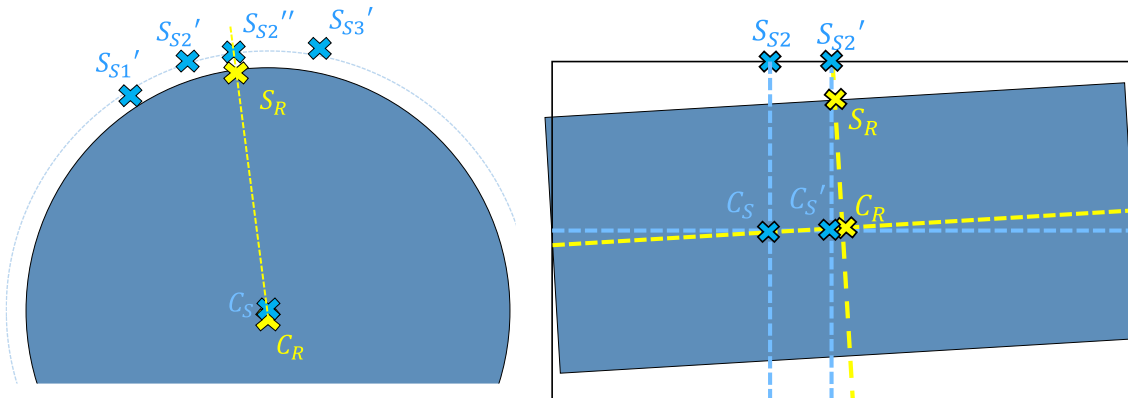
Figure 4:   Schematic view of rotor (dark blue) with rotor markers (yellow) and stator (transparent) for determining the smallest air gap widths for S_R.

For the stator force application for the marker S_{S2} a similar algorithm is used, shown in Figure 5:

1. Calculate the line equation between S_S and C_S
2. Select the nearest rotor maker S_R
3. Project the corresponding rotor center point C_R into the plane of S_S and C_S to get C_R'
4. Determine S_R' with the circle radius of $\overrightarrow{C_R S_R}$
5. Rotate the circle of S_R' and C_R' with the inclination angle to get ellipse equation
6. Calculate the intersection point between the ellipse and $\overrightarrow{S_{S2} C_S}$ to get S_R''

Depending on this local air gap width and the angular position of rotor and stator the respective forces are applied to this individual marker. The amplitude of these forces (radial and tangential) are stored within a look-up table. This look-up table is fed with the solution of electromagnetic finite-element solutions, which is introduced in the following section.
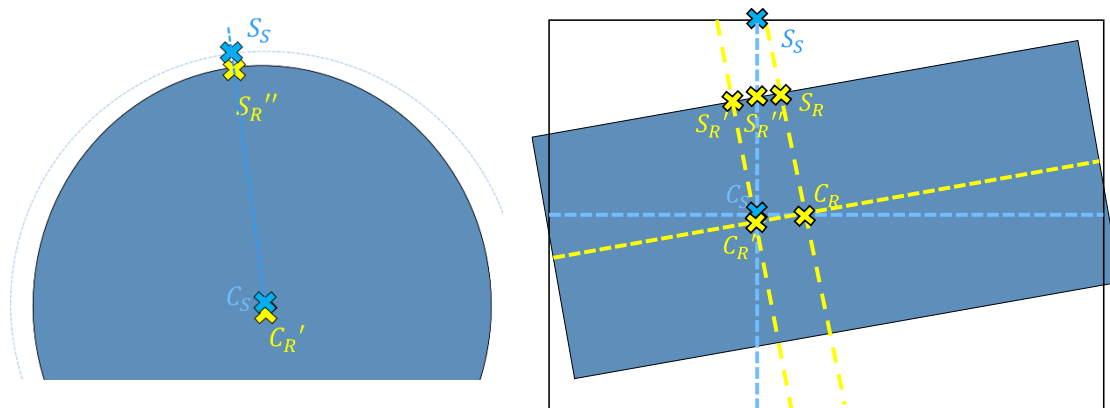
Figure 5: Schematic view of rotor (dark blue) with rotor markers (yellow) and stator (transparent) for determining the smallest air gap widths for S_S.

4. Electromagnetic calculation: Air gap field and forces

Beside the tangential force acting on the rotor of the generator as utilizable torque, radial forces are excited by magnetic flux density waves. As initially introduced, these electromagnetic excited forces have a parasitic impact on structural components of the turbine. The force densities can be derived from the well-known Maxwell stress tensor and are calculated where B_{rad} and B_{tan} are the magnetic flux density components in radial and tangential direction respectively depending on time t and circumferential coordinate x:

$$\sigma_{\mathrm{rad}}(x,t) = \frac{1}{2\mu_0}\left(B_{\mathrm{rad}}^2(x,t) - B_{\mathrm{tan}}^2(x,t)\right)$$
$$\approx \frac{1}{2\mu_0}B_{\mathrm{rad}}^2(x,t), \tag{1}$$

$$\sigma_{\mathrm{tan}}(x,t) = \frac{1}{\mu_0}B_{\mathrm{rad}}(x,t)\,B_{\mathrm{tan}}(x,t). \tag{2}$$

In (2), it is assumed that $B_{\mathrm{rad}} \gg B_{\mathrm{tan}}$.

The force excitation of the structural elements can be calculated by surface integrals over the structural areas adjacent to the air gap of the generator. In the case of the stator, the teeth of the electrical steel core conducting the magnetic flux exert these forces.

Air gap imperfections resulting from wind loads, inhomogeneous thermal conditions or manufacturing tolerances of the machine will change the local magnetic field distribution. In Figure 6, schematic illustrations of a protruding pole and a static eccentricity are shown. Both effects lead to a deviation $\epsilon(\varphi)$ from the ideal air gap width δ_0 and therefore to the air gap width distribution $\delta(\varphi)$, depending on the circumferential position determined by the angle φ:

$$\epsilon(\varphi) = \delta_0 - \delta(\varphi). \tag{3}$$

Predictive models must take these effects into account, since they have a significant impact on the electromagnetically excited forces [8]. The air gap width distribution represents accordingly one dimension of the shown look-up table-based method.

In the course of this work, an electrically excited synchronous generator with salient poles is studied. The stator feeds a DC-link converter (full-scale). The rotor winding of this machine topology is fed with a variable direct current I_f exciting the magnetic rotor field of the machine. Since this quantity depends
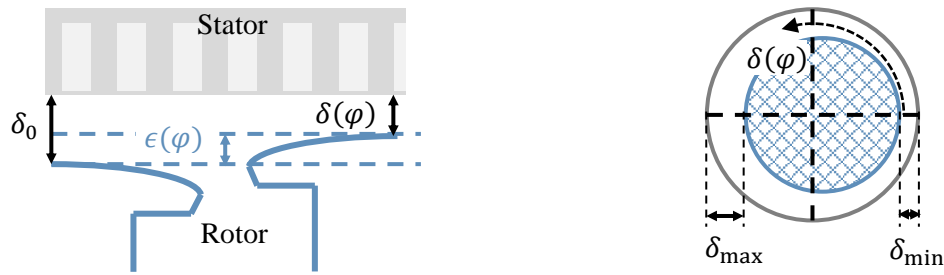
Figure 6:   Schematic illustration of protruding poles (left) and static eccentricity (right).

on the dynamic operating point of the wind turbine (rotational speed) controlling both, the induced voltage and torque of the electric machine, it is another variable of the table utilized by the force element. Static electromagnetic 2D-finite element analysis of a partial model of the machine by using symmetry properties for one electric period has been performed. The air gap flux density as well as tooth forces are evaluated to study the impact of the stated geometric and electric quantities. A schematic illustration of stator with zoomed tooth and results of quantities are illustrated in Figure 7 (above). The indicated force exertion point represents one marker of the force element following the method introduced in the previous section. Its geometric location is defined based on the proposed method and represents the interface between electromagnetic and structural dynamic calculation.

In the diagrams in Figure 7 (below), the normalized magnetic flux density in the air gap b_δ (left) and tooth force f (right) in radial (dot-dashed line) and tangential direction (solid line) are illustrated respectively.
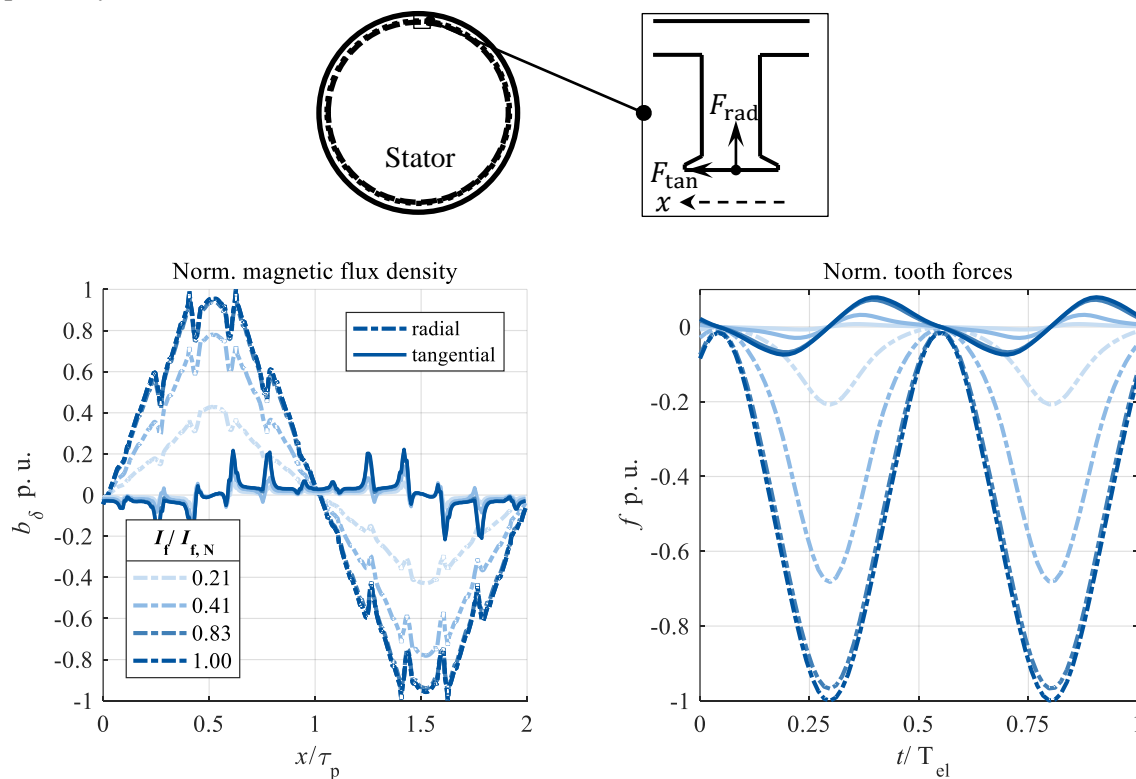
Figure 7:   *Above*: Schematic illustration of a stator with a zoomed tooth (forces indicated).
                   Below: No-load results for magnetic air gap flux density (left) and tooth forces (right).
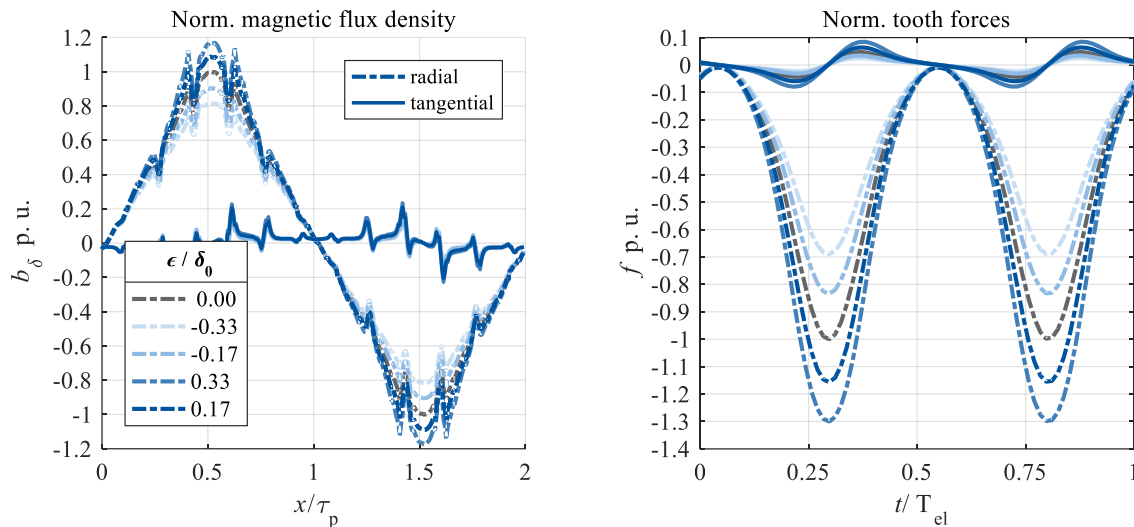
Figure 8:   No-load results (at $I_f = 0.41\,I_{f,N}$) for magnetic air gap flux density and tooth forces in radial and tangential direction for different air gap widths.

The local magnetic field distribution (over two pole pitches of one rotor position) and time curve (for one electric period) of tooth forces are evaluated for different excitation currents (related to its rated value $I_{f,N}$ as indicated in the legend) in no-load condition.

Thereby its sensitivity can be studied separated from the stator current (load-dependent) towards the field excitation for the ideal machine geometry. The results for the coupled simulation of the exciting forces can be examined in the context of the proposed approach.

The magnetic field analysis show that for small excitation currents or rather small magnetic field strengths ($I_f/I_{f,N} \le \mathbf{0.41}$) the magnetic flux increases approximately linear and therefore the radial force even higher (compare to (1)). The sensitivity of the magnetic flux density in magnetically saturated state (two other lines) towards the excitation field strength is less pronounced as expected. However, the radial force exerted by the stator teeth increases by approximately 3 %.

In Figure 8 the no-load results for a constant excitation current and different air gap widths are illustrated. The relative deviation ϵ/δ_0 from the ideal air gap width is varied between +/- 33.3… % and is assumed to be constant in circumferential direction. The maximum magnetic flux density differs by about +/- 20 %, the maximum radial tooth force even by approximately +/- 30 %. The results are stored in the look-up table and can be used to take air gap imperfections into account.

5. Experimental validation: Test bench measurements

To validate the proposed model approach, a 4 MW full-size wind-turbine test bench will be used [9]. Electrical and mechanical quantities as e.g. generator currents and surface accelerations are measured to determine the correlation between electromagnetic excited forces and the structural dynamic response. In Figure 9 the test bench setup with a device under test (DUT), representing a direct-drive topology, is illustrated. Besides the operating characteristics, namely the power and speed curve depending on the averaged hub wind speed of the DUT are shown.

Different load points are studied to identify critical speeds with correlating generator magnetic field frequencies exciting the structure. Particularly at partial load, the rotational speed varies as indicated by the speed curve. Beside parasitic radial forces, the impact of increasing torque causing dynamic tangential forces (shear stress) on the rotor and stator of the generator is particularly relevant in the range of full-load operation. Finally, dynamic loads resulting from turbulent wind conditions are studied to evaluate the sensitivity of structural dynamics towards air gap deformations.
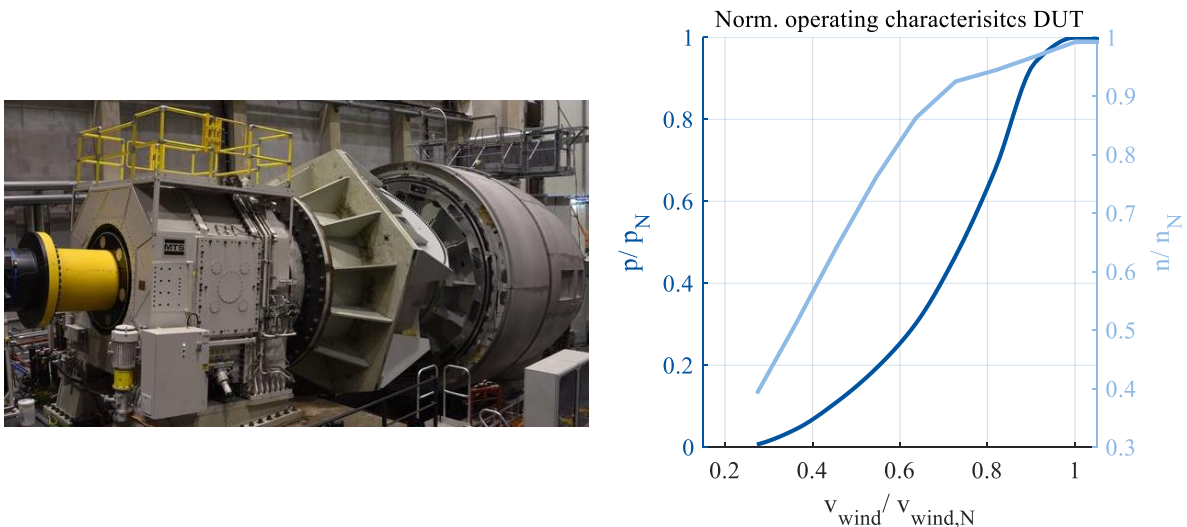
Figure 9: Test bench setup with DUT and normalized operating characteristics of DUT (average wind speed vs. power and rotational speed).

6. Conclusion and Outlook

In this paper a multi-physical modelling approach for direct-drive generators is presented. First the electromechanical model interaction via a force-element is shown. The method for determining the marker points for force coupling are explained geometrically with projection planes. Hereby, deformations and rotor displacements, as e.g. tilting and eccentricities, can be described in the force element. Furthermore, no-load results for the flux density distribution and stator tooth forces in the electrically excited synchronous generator are shown. Its sensitivity towards the excitation current and air gap width is explained. These quantities are therefore variables in the look-up table representing the interface between the force element and the electromagnetic model.

In future work, load-dependent vibrations in direct-drive wind generators will be analysed by the presented look-up table-based force element method. Different air gap imperfections and its impact on the structural dynamic behaviour of the wind turbine will be under the scope of this research. An experimental study by means of a 4 MW full scale test bench is additionally intended to validate the proposed model approach.

7. Acknowledgement

References

[1] R. Wiser, et al.; "Reducing wind energy costs through increased turbine size: Is the sky the limit." Rev. Berkeley National Laboratory Electricity Markets and Policy Group (2016).

[2] A. Binder: Elektrische Maschinen und Antriebe. Berlin, Heidelberg: Springer Berlin Heidelberg, 2017.

[3] Dassault Systemes Simulia Corp.: Simpack Documentation (2020).

[4] T. Duda; G. Jacobs; D. Bosse; Electromechanical Simulation of a Direct – Drive Generator Considering Parasitic Magnetic Forces and External Loads; in: Conference for Wind Power Drives 2019 Conference Proceedings; Rik De Doncker, Kay Hameyer, Georg Jacobs, Antonello Monti, Wolfgang Schröder; Aachen 2019.

[5] T. Duda; G. Jacobs; D. Bosse; "Investigation of Modelling Depths for an Electromechanical Simulation of a Direct-Drive Generator Considering Parasitic Airgap Forces and External Loads"; in: Wind Europe Conference and Exhibition 2019, Bilbao; 2019.

[6] M. Mueller and A. Zavvos; "Electrical generators for direct drive systems: a technology overview," in Electrical drives for direct drive renewable energy systems: Elsevier, 2013, pp. 3–29.

[7] S. Rick; M. Oberneder; K. Hameyer; "Torsional vibrations in multi-megawatt wind turbine induction generators"; Conference for Wind Power Drives 2017: Tagungsband zur Konferenz; Books on Demand; 2017.

[8] C. Mülder, M. Franck, M. Schröder, M. Balluff, A. Wanke, and K. Hameyer; "Impact Study of Isolated and Correlated Manufacturing Tolerances of a Permanent Magnet Synchronous Machine for Traction Drives," in 2019 IEEE International Electric Machines & Drives Conference (IEMDC), 2019, pp. 982–987.

[9] N. R. Averous et al., "Development of a 4 MW full-size wind-turbine test bench," IEEE journal of emerging and selected topics in power electronics, vol. 5, no. 2, pp. 600–609, 2017.